

Designing aspects of photoacoustic cell for crystalline solids

A.P. Sarode¹✉, O.H. Mahajan²

¹Dr. A.G.D. Bendale Girls College, Jhilla Road, Jalgaon 425002, India

²M.J. College, Jalgaon 425001, India

✉ abhisarode@rediffmail.com

Abstract. Today, non-destructive analysis techniques for solids are playing an important role in industrial applications and scientific as well as technological research. Photoacoustic method is one of such non-destructive methods, in which generation of acoustic waves takes place due to the absorption of the modulated incident radiation. Photoacoustic cell is a base for photoacoustic research. Hence design and performance optimization play an important role in determining the efficiency of that cell. The design of the photoacoustic cell depends on various aspects like mode of operation, thermal diffusion, nature of the radiation source, and type of the detector. In this paper, designing aspects of a new photoacoustic cell for crystalline solids are presented. A mathematical expression for population density of absorbing molecules in the excited state of a crystalline solid during photoacoustic interaction in terms of the radiative and collisional time constants is also determined.

Keywords: crystalline solids, photoacoustic transducers, photoacoustic testing, photoacoustic effect, photoacoustic cell

Acknowledgements. *Granted in VCRM Scheme of K.B.C.N.M. University, Jalgaon, India.*

Citation: Sarode AP, Mahajan OH. Designing aspects of photoacoustic cell for crystalline solids. *Materials Physics and Mechanics*. 2022;50(1): 184-191. DOI: 10.18149/MPM.5012022_14.

1. Introduction

Photoacoustic effect is based on the absorption of electromagnetic radiation by analyte molecules [1]. Non-radiative relaxation processes, such as collisions with other molecules, lead to local warming of the sample matrix [2,3]. Pressure fluctuations are then generated by thermal expansion, which can be detected in the form of acoustic or ultrasonic waves. In other words, the transformation of an optical event to an acoustic one takes place in photoacoustic effect. A fraction of the radiation falling upon the sample is absorbed and results in excitation, the type of which is being dependent upon the energy of the incident radiation.

Photoacoustic technique is applicable to solids, liquids, and gases. It is a robust and sensitive technique used today for analysis. The cells used in this technique are widely studied by researchers in the last decade. Chrobak and Malinski presented design of a new photoacoustic cell and its performance optimisation in 2013 [4]. Photoacoustic cell based on Helmholtz resonances was demonstrated by M.N. Popovik et al. in 2016 [5]. In the same year, design framework for an open photoacoustic cell was given by B. Lang and A. Bergman [6]. In 2017, Bluvshstein et al. presented calibration of a multiple pass photoacoustic cell using light-absorbing aerosols [7]. Optical frequency comb photoacoustic detection was presented by Sadiiek et al. in 2018 [8]. In recent years, Cotterell et al. gave optimisation of the performance of aerosol photoacoustic cells in 2019 [9]. In the same year, Sathiyamoorthy and

Kolios demonstrated experimental design and numerical investigation of a photoacoustic cell for microscopic applications [10]. Last year, Said El-busaidy et al. presented modelling of open photoacoustic cell [11].

The cells in photoacoustic spectroscopy are small cylindrical cavities where the radiation interacts with the target material [12]. The radius of the cavity is limited by the size of the infrared beam. The length of the photoacoustic cell is generally as small as possible. On the other hand, a longer absorption length would lead to a larger signal and better signal-to-noise ratio. The photoacoustic cell design also affects the signal generation by defining the heat conduction out of the cell. Therefore it is essential to consider the thermal effects in the cell. The other important aspects are mode of operation, shape of the cell, modulation scheme, and heat absorption in the crystal.

2. Processes in photoacoustic cell

Non-radiative de-excitation processes which normally occur in the cell, give rise to the generation of thermal energy within the sample [13]. If the incident radiation is modulated then the generation of thermal energy within the sample will also be periodic and a thermal wave or a pressure wave will be produced having the same frequency as this modulation. Energy is transferred by the thermal wave or the pressure wave towards the sample boundary, where a periodic temperature change is generated [14]. The periodic variation in the temperature at the surface of the sample results in the generation of an acoustic wave in the gas immediately adjacent and this wave propagates through the volume of the gas to the detector (microphone, piezoelectric transducers, or optical method) where a signal is produced [15]. This detector or microphone signal, when plotted as a function of wavelength, will give a spectrum proportional to the absorption spectrum of the sample.

3. Aspects of designing

The important aspects of designing of a photoacoustic cell for a solid crystal are

- 1) Mode of Operation
- 2) Scheme of Excitation
- 3) Shape of the cell
- 4) Heat Absorption in the crystal

Mode of operation. In a closed photoacoustic cell, the enclosed air surrounding the crystal will vibrate as per the modulating frequency of the source of incident radiation. When the mode of operation is resonant, one of the resonant frequencies of the signal in the cavity will be the modulation frequency of the incident source. The pressure fluctuations in the cell will generate an acoustic wave whose amplitude will be amplified at the frequency of modulation of the incident radiation. The amplification of the signal will be proportional to quality factor Q . Quality factor represents relation between resonant frequency of the signal and its bandwidth. To amplify only the modulating frequency of the generated signal inside the cell, a large separation should be kept between the adjacent resonance frequencies along with a high-quality factor [16]. The amplification of all other remaining resonant frequencies will be inversely proportional to the subtraction between the square of the modulating frequency and the square of the resonant frequency of the generated signal.

If the mode of operation of photoacoustic cell used is resonant then implemented modulation frequencies are relatively high, around 3 kHz. The purpose of this selection is to minimize the noise depending on the reciprocal of the frequency. The associated noises are external acoustic noise, noise due to amplification, and intrinsic noise of the detector. The cavity length is shorter for higher frequencies. Hence while selecting the resonant frequency, an intermediate value between a longer absorption length and shorter cavity length should be

preferable. Generally, a smaller cavity length is preferred so as to have a compact cell having a shorter response time [17].

Scheme of excitation. As mentioned earlier, the photoacoustic effect is based on the sample heating produced by optical absorption. In order to generate acoustic waves, which can be detected by pressure-sensitive transducers, periodic heating and cooling of the sample is necessary to generate pressure fluctuations.

Modulated excitation. In modulated excitation schemes, radiation sources are employed whose intensity fluctuates periodically in the form of a square or a sine wave, resulting in a 50% duty cycle. This can be realized for example by the mechanical chopping of a light source. A way to overcome the 50% duty cycle is to modulate the phase instead of the amplitude of the emitted radiation. On the other hand, chopped or modulated lamps or IR sources from commercial spectrometers are used for the determination of UV or IR absorption spectra of opaque solid crystals [18]. Modulated continuous wave lasers are the most common sources for photoacoustic analysis. Photoacoustic cell play an important role in photoacoustic effect. This fact can be utilized for signal enhancement by acoustic resonance. Thus, acoustic resonance curves must be considered in photoacoustic cell design.

Pulsed excitation. In pulsed photoacoustic spectroscopy, laser pulses with durations in the nanosecond range are usually employed for excitation. Since the repetition rates are in the range of a few Hz, the result is a short illumination followed by a much longer dark period: a low-duty cycle. This leads to a fast and adiabatic thermal expansion of the sample medium resulting in a short shock pulse. Data analysis in this case is performed in the time domain. Therefore, the signal is recorded by oscilloscopes, boxcar systems, or fast A to D converters. Transformation of the signal pulse into the frequency domain results in a wide spectrum of acoustic frequencies up to the ultrasonic range [19]. Thus, laser beams modulated in the form of a sine wave excite one single acoustic frequency, whereas short laser pulses are broadband acoustic sources.

Shape of the cell. Resonant photoacoustic cell is fabricated according to the required dimensions of the internal cavity suitable to the acoustic wavelength [20]. A schematic diagram of cylindrical photoacoustic cell for a solid crystal is shown in Fig. 1. The structure of the cell is modified by connecting additional buffers to the central part as shown. Addition of buffers is useful in the prevention of noise due to the coupling of the cell with the other measurement devices.

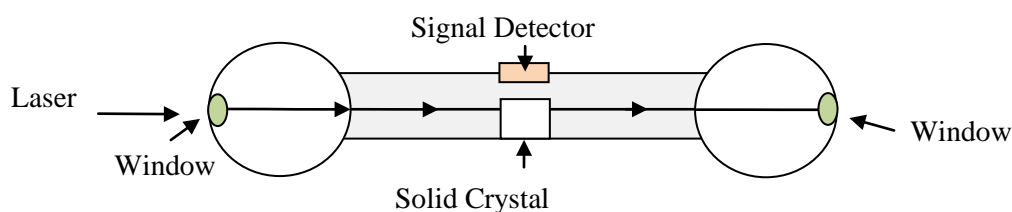


Fig. 1. A schematic diagram of a newly designed photoacoustic cell for a crystalline solid

A resonator with short dimensions oriented in the perpendicular direction with respect to the propagating acoustic signal represents a one-dimensional photoacoustic cell. When the propagating sound waves are reflected back in the cell, standing acoustic waves generated by the excited sound signals are amplified if the difference in phase of the waves is 2π or in its multiple. The reflections of the waves at the ends of the cell as well as acoustic path length are the important factors on which phase difference depends. At the closed end of the cell, a pressure antinode will be formed. The reason for this is the higher acoustic impedance of the cell material than air [21].

The most used shape of the photoacoustic cell is a cylindrical shape because it matches the symmetry of the laser beam. For a small size acoustic sensor or a microphone, the measured signal is proportional to the amplitude of acoustic signal at its location. Unwanted sound signals generated in resonance from the external sources are reduced by placing the sensor at the node of the generated amplified wave. The desired value of the Q factor for a cylindrical photoacoustic cell can be designed up to 900.

Heat absorption in the crystal. For absorbing samples the optical absorption length is an important parameter and may be taken as the depth into the sample at which essentially all of the incident radiation has been absorbed. The thermal wave produced in the sample is heavily damped and may be considered to be fully damped out within a distance of $2\pi\mu_s$, where μ_s is the thermal diffusion length. It is normally assumed that only those thermal waves originating from a depth less than or equal to μ_s will make an appreciable contribution to the photoacoustic signal measured.

The observed photoacoustic signal is a complex quantity having a magnitude and phase relative to the modulation of incident radiation. Being a function of the absorption coefficient, modulation frequency, and thermal characteristics of the sample as well, the photoacoustic signal is directly proportional to the incident power of the radiation and also depends upon the characteristics of the gas in contact with the sample surface and the properties of the backing material upon which the sample is positioned [22].

To describe the absorption of light in a crystalline solid, consider a two-level system, in which energy transfers take place. A schematic representation of a two-level system in a crystal in photoacoustic interaction is shown in Fig. 2. These energy transfers are radiative and non-radiative. Let us consider two states i and j . Also, consider the coefficients r_{ij} and c_{ij} . The radiative transition rate is r_{ij} and c_{ij} is non-radiative transition rate c_{ij} is also called collision-induced energy transfer. Now, introduce Einstein coefficients for stimulated and spontaneous emission, B_{ij} and A_{ij} . Consider ρ_ω as the spectral energy density at the frequency of the transition between E_0 and E_3 . Einstein coefficients can be expressed as

$$r_{ij} = \rho_\omega B_{ij} + A_{ij}, \quad (1)$$

where ρ_ω is the spectral energy density at the frequency of the transition between E_0 and E_3 . The quantity ρ_ω measures the radiant energy per volume per unit frequency and can be expressed in terms of units Js / m^3 .

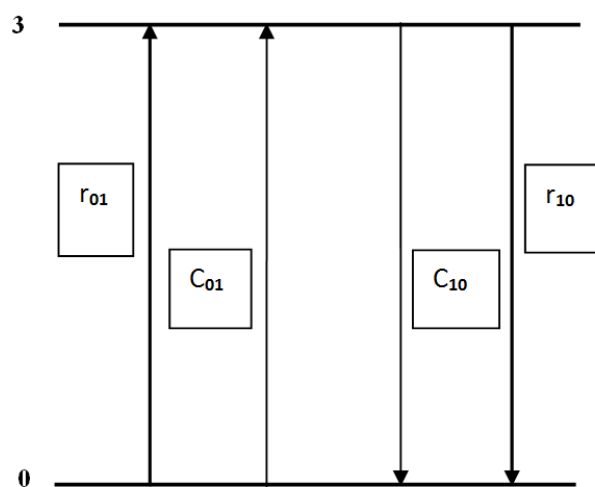


Fig. 2. A schematic representation of a two-level system in a crystal

Note that $B_{ij} = B_{ji}$ so that $B_{03} = B_{30}$. But $A_{03} = 0$ because spontaneous emission from a state of lower energy to any one of higher energy does not occur.

Hence, $r_{03} = \rho_{\omega} B_{03}$.

Also, $r_{30} = \rho_{\omega} B_{03} + A_{30}$.

Again, the probability of excitation due to collision from E_0 to E_3 is very low. Therefore, approximately we can say,
 $c_{03} \approx 0$.

Let us determine the rate of transition. For this calculation, we must distinguish the population densities of absorbing molecules in the ground and excited states. Consider these population densities as n_0 and n_3 , respectively corresponding to energies E_0 and E_3 . To calculate the rate of change of population in the upper state, we must consider the difference between the number of molecules entering and leaving the excited state.

$$\begin{aligned} \dot{n}_3 &= (r_{03} + c_{03})n_0 - (r_{30} + c_{30})n_3, \\ \dot{n}_3 &= \rho_{\omega} B_{03} n_0 - (\rho_{\omega} B_{03} + A_{30} + c_{30})n_3, \\ \dot{n}_3 &= \rho_{\omega} B_{03} n_0 - \rho_{\omega} B_{03} n_3 - (A_{30} + c_{30})n_3, \\ \dot{n}_3 &= \rho_{\omega} B_{03} (n_0 - n_3) - (A_{30} + c_{30})n_3. \end{aligned} \quad (2)$$

Let the radiative and collision time constants be $T_r = \frac{1}{A_{30}}$ and $T_c = \frac{1}{C_{30}}$ respectively.

The total time constant is, then the addition of radiative and collision time constants.

$$T = T_r + T_c.$$

Now, equation (3) can be written as

$$\dot{n}_3 = \rho_{\omega} B_{03} (n_0 - n_3) - \left(\frac{1}{T_r} + \frac{1}{T_c} \right) n_3. \quad (3)$$

Let us follow a similar process to calculate \dot{n}_0 as

$$\begin{aligned} \dot{n}_0 &= (r_{30} + c_{30})n_3 - (r_{03} + c_{03})n_0, \\ \dot{n}_0 &= (\rho_{\omega} B_{03} + A_{30} + c_{30})n_3 - \rho_{\omega} B_{03} n_0, \\ \dot{n}_0 &= \rho_{\omega} B_{03} (n_3 - n_0) + (A_{30} + c_{30})n_3, \\ \dot{n}_0 &= \rho_{\omega} B_{03} (n_3 - n_0) + (+)n_3, \\ \dot{n}_0 &= \rho_{\omega} B_{03} (n_3 - n_0) + \left(\frac{T_r + T_c}{T_r T_c} \right) n_3. \end{aligned} \quad (4)$$

Hence,

$$\begin{aligned} \dot{n}_3 - \dot{n}_0 &= \rho_{\omega} B_{03} (n_0 - n_3) - \left(\frac{1}{T_r} + \frac{1}{T_c} \right) n_3 - \left[\rho_{\omega} B_{03} (n_3 - n_0) + \left(\frac{T_r + T_c}{T_r T_c} \right) n_3 \right], \\ \dot{n}_3 - \dot{n}_0 &= \rho_{\omega} B_{03} (n_0 - n_3) - \left(\frac{1}{T_r} + \frac{1}{T_c} \right) n_3 - \rho_{\omega} B_{03} (n_3 - n_0) - \left(\frac{T_r + T_c}{T_r T_c} \right) n_3, \\ \dot{n}_3 - \dot{n}_0 &= \rho_{\omega} B_{03} n_0 - \rho_{\omega} B_{03} n_3 - \left(\frac{1}{T_r} + \frac{1}{T_c} \right) n_3 - \rho_{\omega} B_{03} n_3 + \rho_{\omega} B_{03} n_0 - \left(\frac{T_r + T_c}{T_r T_c} \right) n_3, \\ \dot{n}_3 - \dot{n}_0 &= 2\rho_{\omega} B_{03} n_0 - 2\rho_{\omega} B_{03} n_3 - 2 \left(\frac{T_r + T_c}{T_r T_c} \right) n_3, \end{aligned}$$

$$\dot{n}_3 - \dot{n}_0 = -2 \left\{ \rho_\omega B_{03} (n_3 - n_0) + \left(\frac{T}{T_r T_c} \right) n_3 \right\}. \quad (5)$$

To consider an interchange adiabatically in upper and lower population in steady state condition, intensity, I should vary slowly. In such situation, we can say that

$$\dot{n}_3 - \dot{n}_0 = 0.$$

So equation (5) becomes

$$0 = -2 \left\{ \rho_\omega B_{03} (n_3 - n_0) + \left(\frac{T}{T_r T_c} \right) n_3 \right\}.$$

We know that total molecular density is

$$N = n_0 + n_3,$$

$$n_3 = N - n_0,$$

$$0 = -2 \left\{ \rho_\omega B_{03} (N - n_0 - n_0) + \left(\frac{T}{T_r T_c} \right) n_3 \right\},$$

$$0 = -2 \left\{ \rho_\omega B_{03} (N - 2n_0) + \left(\frac{T}{T_r T_c} \right) n_3 \right\},$$

$$0 = -2 \rho_\omega B_{03} (N - 2n_0) - 2 \left(\frac{T}{T_r T_c} \right) n_3,$$

$$0 = -2 \rho_\omega B_{03} N + 4 \rho_\omega B_{03} n_0 - 2 \left(\frac{T}{T_r T_c} \right) n_3,$$

$$4 \rho_\omega B_{03} n_0 = 2 \rho_\omega B_{03} N + 2 \left(\frac{T}{T_r T_c} \right) n_3,$$

$$n_0 = \left\{ 2 \rho_\omega B_{03} N + 2 \left(\frac{T}{T_r T_c} \right) n_3 \right\} / 4 \rho_\omega B_{03},$$

$$n_0 = \left\{ \rho_\omega B_{03} N + \left(\frac{T}{T_r T_c} \right) n_3 \right\} / 2 \rho_\omega B_{03}, \quad (6)$$

and,

$$n_3 = \left\{ 4 \rho_\omega B_{03} n_0 - 2 \rho_\omega B_{03} N \right\} / 2 \left(\frac{T}{T_r T_c} \right),$$

$$n_3 = \left\{ 2 \rho_\omega B_{03} n_0 - \rho_\omega B_{03} N \right\} / \left(\frac{T}{T_r T_c} \right). \quad (7)$$

Thus, population density of absorbing molecules in the excited state during photoacoustic interaction of a solid crystal is exactly determined.

4. Conclusions

Thus, a mathematical expression for population density of absorbing molecules in the excited state during photoacoustic interaction in terms of the radiative and collisional time constants for a crystalline solid is exactly determined. This expression allows the calculation of various parameters of photoacoustic signal related with solid crystal in the designed photoacoustic cell. The cell designing in terms of heat absorption in the crystal, mode of operation, scheme of excitation, and shape of the cell is theoretically presented. This theoretical approach constitutes an important step towards determination of various aspects of new designs of

photoacoustic cells for solid crystals. This work will be useful in photoacoustic research for scientific and industrial applications in various fields in the future.

References

1. Rosencwaig A, Gersho A. Theory of Photoacoustic effects in solid. *Journal of Applied Physics*. 1976;47(1): 64-67.
2. West G, Barrett JJ, Siebert DR, Reddy KV. Photoacoustic Spectroscopy. *Review of Scientific Instruments*. 1983;54(7): 797-817.
3. McDonald FA, Wetsel GC. Generalized Theory of the Photoacoustic Effect. *Journal of Applied Physics*. 1978;49(4): 2313-2322.
4. Chrobak L, Malinski M. Design and optimization of the photoacoustic cell for nondestructive photoacoustic spectroscopy. *Nondestructive Testing and Evaluation*. 2013;28(1): 17-27.
5. Popovic MN, Nestic MV, Ciric-Kostic S, Zivanov M, Markushev DD, Rabasovic MD, Galovic SP. Helmholtz Resonances in Photoacoustic Experiment with Laser-Sintered Polyamide Including Thermal Memory of Samples. *Int J Thermophys*. 2016;37: 116.
6. Lang B, Bergmann A. Design framework for a gas sensor based on an open photoacoustic resonator. *IEEE Sensors*. 2016;4: 1-3.
7. Bluvshstein N, Flores JM, He Q, Segre E, Segev L, Hong N, Donohue A, Hilfiker JN, Rudich Y. Calibration of a multi-pass photoacoustic spectrometer cell using light-absorbing aerosols. *Atmos. Meas. Tech*. 2017;10(3): 1203-1213.
8. Sadiq I, Mikkonen T, Vainio M, Toivonen J, Foltynowicz A. Optical frequency comb photoacoustic spectroscopy. *Physical Chemistry Chemical Physics*. 2018;20(44): 27849-27855.
9. Cotterell MI, Ward GP, Hibbins AP, Wilson A, Langridge JM. Optimizing the performance of aerosol photoacoustic cells: Method validation and application to single-resonator multipass cells. *Aerosol Science and Technology*. 2019;53(10): 1107-1127.
10. Sathiyamoorthy K, Kolios MC. Experimental design and numerical investigation of a photoacoustic sensor for a low-power, continuous-wave, laser-based frequency-domain photoacoustic microscopy. *Journal of Biomedical Optics*. 2019;24(12): 121912.
11. El-Busaidy SAS, Baumann B, Wolff M, Duggen L. Modelling of open photoacoustic resonators. *Photoacoustics*. 2020;18: 100161-100164.
12. Wolff M, Harde H. Photoacoustic Spectrometer Based on a Planckian Radiator with Fast Time Response. *Infrared Physics & Technology*. 2003;44(1): 51-55.
13. Kottmann J, Rey JM, Sigrist MW. New photoacoustic cell design for studying aqueous solutions and gels. *Rev. Sci. Instrum*. 2011;82(8): 084903.
14. Malinski M. Determination of air-tightness of the packaging of electronic devices by the thermoacoustic method. *Arch. Acoust*. 2005;30(3): 345-355.
15. Wilcken K, Kauppinen J. Optimization of a Microphone for Photoacoustic Spectroscopy. *Applied Spectroscopy*. 2003;59(9): 1087-1092.
16. Tavakoli M, Tavakoli A, Taheri M, Saghafifar H. Design, simulation and structural optimization of a longitudinal acoustic resonator for trace gas detection using laser photoacoustic spectroscopy. *Opt. Laser Technology*. 2012;42(5): 828-838.
17. Raghu O, Philip J. A dual channel photoacoustic cell for imaging experiments on solid samples. *Journal of the Instrument Society of India*. 2003;33(3): 155-158.
18. Chrobak L, Malinski M. Transmission and absorption based photoacoustic methods of determination of the optical absorption spectra of Si samples – comparison. *Solid State Commun*. 2009;149(39-40): 1600-1604.
19. Rabasovic MD, Nikolic JD, Markushev DD, Jovanovic KJ. Pulsed photoacoustic gas cell design for low pressure studies. *Opt. Mater*. 2008;30(7): 1197-1200.

20. Jorge MPPM, Mendes FJ, Oliveira AC, Braga AJP, Cesar CL, Morato SP, Vieira JrND, Vieira MMF. Resonant photoacoustic cell for low temperature measurements. *Cryogenics*. 1999;39(3): 193-195.
21. Yehya F, Chaudhary AK. Designing and modeling of efficient resonant photoacoustic sensors for spectroscopic applications. *Journal of Modern Physics*. 2011;2: 200-209.
22. Schmid T. Photoacoustic Spectroscopy for Process Analysis. *Analytical and Bioanalytical Chemistry*. 2006;384: 1071-1072.

THE AUTHORS

Sarode A.P.

e-mail: abhisarode@rediffmail.com

ORCID: 0000-0003-4638-1614

Mahajan O.H.

e-mail: abhi.jjit@rediffmail.com

ORCID: 0000-0001-6651-8089